Chapter

Advanced Optical Diagnostics of Atmospheric Pressure Plasma

Qing Xiong

Abstract

Atmospheric-pressure plasma has been employed in various applications including bio-medicine, environmental pollution control, material processing. Diagnostic characterization of plasma sources is critical and indispensable for plasma control and achieving optimized treatment efficiency. In this chapter we will introduce several advanced optical techniques to visualize the detailed physical-and-chemical properties of atmospheric-pressure discharges. Non-invasive approaches of optical emission spectroscopy (OES), schlieren or shadowgraph, invasive methods of active laser spectroscopy including laser-induced fluorescence (LIF), laser or broadband absorption, cavity ring-down spectroscopy (CRDS), and laser scattering are illustrated. Basic plasma parameters of gas temperature, electron density and temperature, electric field strength, and reactive chemical gaseous species (O, H, N, OH, NO, O_3, etc.) are able to be monitored. Comparisons and comments of these approaches are provided depending on diagnostic purposes.

Keywords: advanced optical techniques, plasma parameters, active laser spectroscopy, LIF, absorption spectroscopy

1. Introduction

Atmospheric pressure plasmas attract intensely interests because of non-need of costly vacuum requirement and enabling in-line processing. Prospective novel applications have emerged over recent years, e.g., plasma bio-medicine, material synthesis, pollutant degradation, chemical conversion. However, with increase of gas pressure, plasmas tend to become constricted, unstable, and non-uniform. Miniaturization of discharge volume with non-equilibrium kinetic property are typically characterized by atmospheric pressure plasmas. And in many cases they are of strong gradients in space and in time as well, e.g., the so-called microplasmas. Much higher diagnostic requirements are put forward to atmospheric pressure plasmas with high time-and-space resolution. Not only the traditional optical emission spectroscopy (OES) accessing emitting species, but also advanced active diagnostics particularly the laser-aided techniques probing plasma parameters (T_g, n_e, T_e) and reactive plasma species, are the topics discussed in this chapter.

2. Diagnostics of basic plasma parameters

Plasma parameters mainly are the gas temperature T_g, electron density n_e and temperature T_e. The three are important physical factors directly influencing the

plasma generation and physical-and-chemical properties. Diagnostics of the three parameters are necessary in plasma field from points of both fundamental research and applications.

2.1 Gas temperature

From points of both fundamental investigation and applications, gas temperature (T_g) is one of the important basic plasma parameters strongly affecting the discharge property, especially the plasma chemistry as most chemical reactions are temperature dependent, and thus influences the final outcomes of plasma applications. Standard direct approach by thermocouples is difficult due to induced strong effects on plasma properties. Although thermometric probes based on fiber-optics are developed and applied to plasma diagnostics [1], the use of this technique is still rare and limited to, e.g., microplasmas.

Rotational distributions of molecules, typically from excited molecules are often used to estimate the plasma gas temperature, if the former achieves an equilibrium Boltzmann distribution [2, 3]. In this case the distribution of interested rotational manifold can be estimated from corresponding emissions in UV to visible range and easy to be detected by a spectrometer. Excited species $OH(A^2\Sigma^+)$ and $N_2(C^3\Pi_u)$ are often used for the purpose of T_g estimation, by using programs of Lifbase or SpecAir [4, 5]. However, it needs to keep in mind that, on one hand this method is strongly affected by the production process of excited molecular state. Its rotational population distribution may highly deviate from thermal equilibrium state. This is typically characterized by atmospheric pressure plasmas, in which fast collisions significantly reduce the lifetime of rotational states and if the rotational energy transfer (RET) process is not fast enough to thermalized all rotational levels, a non-thermalized distribution is resulted. In this case T_g estimation will be not precise and overestimated due to over-populated high rotational states. This situation is often existent in water-contacting discharges if $OH(A^2\Sigma^+)$, or argon discharges if $N_2(C^3\Pi_u)$, are applied for T_g determination [6–9]. In this case, method of Boltzmann plotting may help by using the part of rotational states with small rotational number, as these levels with low rotational energy potential are easily thermalized by RET process [2].

On the other hand, it should mention that the emitting region usually characterizes only a part but not the whole discharge space. Commonly, it corresponds to the hot core of the discharge [10]. Other advanced approaches are desired if the full-space distribution of T_g is needed, for instance to estimate the heat flux of discharge to treated object. Laser scattering techniques such as Rayleigh scattering and Raman scattering, and calibrated schlieren photography are proposed and will be illustrated in this chapter. All these methods depend on the neutral density which directly relates to T_g if the ideal gas principle is valid.

Rayleigh scattering is elastic scattering on heavy species and its signal has the same wavelength as the laser. Its intensity depends proportionally on the scattering cross section, laser intensity, and amount of neutral particles probed in the scatter volume [11–14]. By comparing the scattering signals of plasma off I^R_{off} and plasma on I^R_{on}, the gas temperature is obtained if the gas composition does not vary significantly in the probed volume:

$$T_g = T_{ref} \frac{I^R_{off}}{I^R_{on}} \tag{1}$$

where T_{ref} is the known room temperature when plasma is off. An example of a Rayleigh scattering measurement in a pin-to-pin micro-glow air discharge is shown in **Figure 1**. This technique is favored for capturing the T_g spatial distribution of atmospheric pressure plasmas directly, but still following issues needs to be considered if it is applied:

- Laser-induced breakdown needs to be avoided by using appropriate laser energy. UV laser wavelength is suggested for this purpose, even laser energy is low it still able to produce intense scattering signal as the cross section has a strong wavelength dependence ($\sigma \propto \lambda^{-4}$) [12].

- Mie scattering on dust particles and stray scattering light from electrodes needs to be avoided. Therefore, this technique is quite difficult for probing discharge regions close to electrodes.

- The scattering signal will be weak for helium discharge due to the low Rayleigh cross section of helium atoms.

- Deviation will increase for temperature level above 2000 K as intensity of I_{on}^{R} will be very low in above equation.

Schlieren photography also is applied to measure the gas density gradients and correspondingly, to estimate the gas temperature [15, 16]. The advantage of this approach is achievable of the whole T_g distribution by only one schlieren image, if after calibration. A schlieren image visualizes the deflection of light rays along the optical path. The signal intensity of each pixel on the schlieren image is an integration result of bent light ray which strongly depends on the density distribution of gas species. If the gas composition is known and its spatial gradient is induced by thermal motion, then T_g map is able to be calculated through Abel inverse integral transformation. Symmetric assumption is usually made for the T_g map in non-uniform discharges such as pin-to-pin microplasma. For asymmetric discharges, it

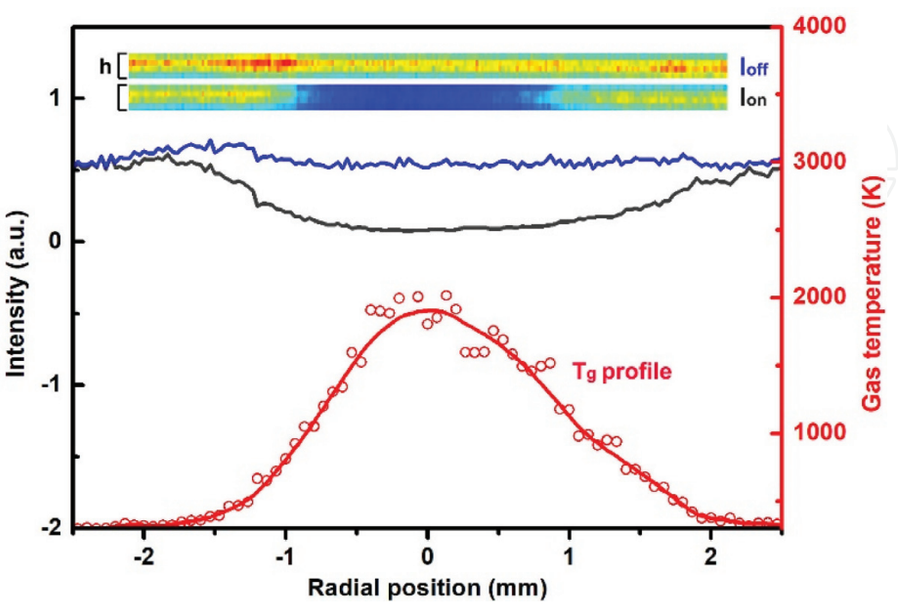

Figure 1.
Radial profiles of Rayleigh scattering intensities when the discharge was off and on, and the estimated gas temperature profile in the middle of discharge column with current of 8 mA [10].

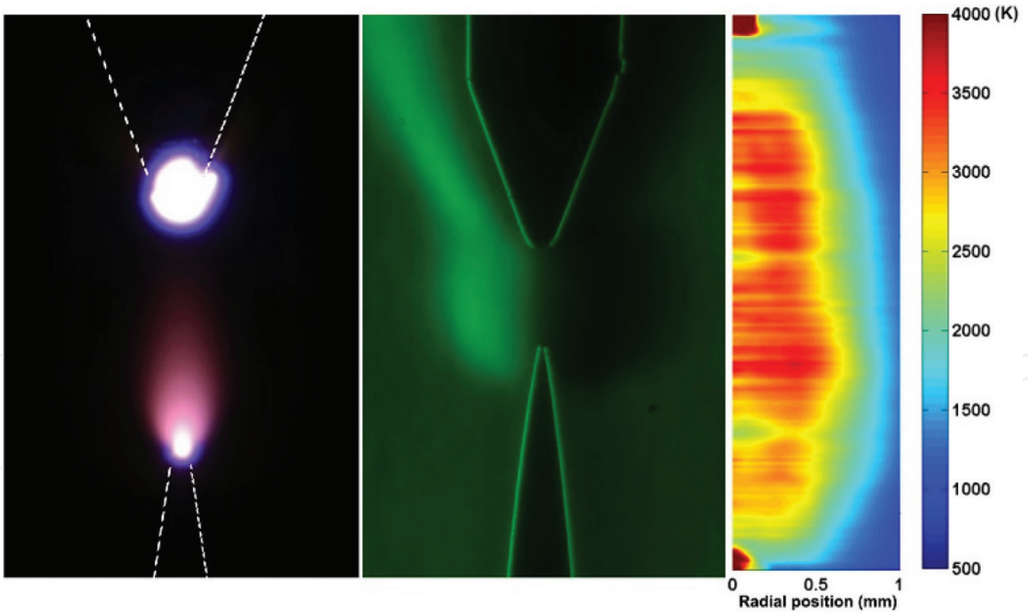

Figure 2.
(From left to right) A pin-to-pin air micro-glow discharge under 16 mA current, its Schlieren image, and two-dimensional T_g map.

is difficult but still possible by a computed tomographic reconstruction technique and multi-directional calibrated Schlieren imaging [16, 17].

Figure 2 shows an example of full T_g map estimated by calibrated schlieren photography [10]. It needs to point out that this technique suffers the optical diffraction effect on the object boundary, which usually induces an overestimation of temperature. However, compared to laser scattering approach, calibrated schlieren is a low-cost way for full-mapping gas temperature in discharges. Its drawback is the calibrated calculation process and need extra calibration by a long-focus lens.

Other methods including Raman scattering also allows one to measure the gas temperature [13]. It is the inelastic scattering of light on molecules such as N_2 or O_2 and its signal depends on neutral density, similar to the Rayleigh scattering. However, this technique requires expensive laser equipment and filter system for removing strong interference of Rayleigh scattering. Doppler broadening and Van der Waals broadening are analyzed for line profiles to estimate T_g as well if the Stark broadening is not dominant [18, 19]. However, the broadening routines require high spectral resolution to reduce the effect from instrumental broadening. Compared to emission lines, fine structure of atomic absorption line is achievable by tunable diode laser absorption measurement [8]. Compared to Doppler broadening, Van der Waals broadening is preferred for atmospheric-pressure plasmas with low gas temperature as the latter depends strongly on the neutral density. It should mention that the both broadening routines are line-integrated measurements and Abel inversion is required if radial profile of T_g is desired. **Table 1** concludes and compares all these methods for T_g diagnostics described above. Two or more techniques are suggested if diagnosing non-uniform high-pressure plasmas.

2.2 Electric-field strength

Electric-field strength E determination is always a tough issue for high-pressure plasmas. Compared to emission spectroscopic methods based on Stark effect of atomic lines, coherent Raman scattering (CRS) technique is favored for both static and fast transient discharges at elevated pressures [22, 23]. Its basic principle is vibrational excitation of Raman-active molecular which produces an infrared (IR)

Methods	Advantages	Disadvantages	Ref.
Rotational temperature of molecules	• Spatial resolution can be high; • Flexible and achievable by a fiber-optics spectrometer	• Line-averaged • Non-equilibrium distribution if quenching is strong • Characterize only radiative region	[2, 3]
Broadenings of line profile	• Spatial resolution can be high; • Non-dependent on quenching process	• Require high-spectral resolution; • Line-averaged	[18, 19]
Rayleigh scattering	• Spatial resolution can be high; • 2D measurement; • Accuracy is high for $T_g < 2000$ K	• Require expensive laser system; • Stray light effect; • Deviation increase for $T_g > 2000$ K	[12–14]
Raman scattering	• Spatial resolution can be high; • 2D measurement	• Require expensive laser system and notch filter	[13, 14]
Schlieren imaging	• Spatial resolution can be high; • Full spatial-field detection	• Need calibration and complex calculation	[10, 15–17, 20, 21]

Table 1.
Summary comparison of various diagnostic techniques for gas temperature determination in atmospheric-pressure discharges.

coherent beam under the effects of two extra nanosecond pulsed laser beams and an electric field. The IR light can be considered as an anti-Stokes wave produced by the electric fields of two laser beams and a third field at zero frequency, i.e., the probed dc electric field [22, 24, 25]. At the same time the laser beams also produce conventional coherent anti-Stokes Raman scattering (CARS) regardless of the presence of the dc electric field. And E is able to be determined from the detected intensities of the two coherent Raman scattering beam, according to:

$$\mathrm{I}_{IR} = \mathrm{C}_1 \left(N_g - N_{ex}\right)^2 I_1 I_2 E^2 \tag{2}$$

$$\mathrm{I}_{CARS} = \mathrm{C}_2 \left(N_g - N_{ex}\right)^2 I_1^2 I_2 \tag{3}$$

$$\mathrm{E}^2 = \frac{\mathrm{C}_2}{\mathrm{C}_1} \frac{\mathrm{I}_1 \mathrm{I}_{\mathrm{IR}}}{\mathrm{I}_{\mathrm{CARS}}} = \mathrm{C}_0 \frac{\mathrm{I}_{\mathrm{IR}}}{\mathrm{I}_{\mathrm{CARS}}} \tag{4}$$

N_g and N_{ex} are the number densities of scattering molecules at the ground and excited levels involved in the vibrational transition. Since the incident laser intensity I_1 is known and can be treated as a constant with two other constants C_1 and C_2. The value of parameter C_0 is almost independent of the gas density or temperature which significantly simplifies the analysis of this technique for E measurement in discharges.

Molecules including N_2 and H_2 have been used as the probe species, particularly the latter due to its large Raman cross section [22, 25]. However, compared to H_2 nitrogen gas has significant potentials for diagnosing atmospheric-pressure discharges especially discharges mixing with nitrogen gas. Based on the four-wave mixing principle of CRS technique by two laser beams, recently a novel and simpler CRS scheme was developed by *I. Adamovich*' group in Ohio State University by using only one laser beam [26–29]. A high-pressure gas cell filled with N_2 and He

with 1:1 mixture ratio was used and pumped by the same laser beam to produce the 607 nm first order Stokes signal of N_2. The 607 nm Stokes beam was generated to replace the need of another nanosecond laser system used in traditional CRS technique. Then the pump and Stokes beams are focused in the discharge region to produce the IR anti-Stokes beam under the presence of probed dc electric field [28]. They applied a picosecond laser at 532 nm especially for probing the transient electric field in nanosecond discharges.

A further simpler approach based on the second harmonic generation (SHG) was developed by the same group for diagnosing the time-resolved evolution of the electric field vector in a nanosecond atmospheric-pressure surface plasma [29]. A single picosecond laser was used without Stokes gas cell. The pump laser wavelength is 1064 nm and focused to the discharge region and under the presence of an external electric field, SHG at 532 nm is generated with intensity proportional to the probed E of discharge [29]. Compared to CRS measurements, this SHG technique involves only one nonlinear optical process which enables better shot-to-shot signal reproducibility and signal/noise level. By using a polarizer in front of the SHG detector the vertical and horizontal components of E in discharge are able to be measured separately. Absolute calibration is required for above all approaches by measuring a known Laplacian electric field between two parallel metal plate electrodes. It should be mentioned that low-frequency nanosecond lasers, such as 10 Hz Nd:YAG pumping laser, is also suitable for E measurement in atmospheric-pressure discharges if ns time-resolution is not required.

2.3 Electron density and temperature

Electron density n_e and temperature T_e are two important fundamental plasma parameters since plasma property is mostly drove by electrons. Stark broadening of atomic line profile is often applied for estimating electron density if n_e typically exceeds 10^{14} cm^{-3} in atmospheric-pressure plasmas. The H_β line is most frequently used for the diagnostic purpose of n_e due to its strong Stark broadening but less self-absorption and weak effect from ion dynamics in discharges [30, 31]. Other hydrogen Balmer lines including H_α and H_γ are also studied and used for n_e determination. The H_α line is more intense of emission but easily suffered self-absorption effects. The Stark broadening of hydrogen Balmer lines has been studied extensively in [32] by group of M. Gigosos. They calculated the line widths of H_β Stark broadening for wide ranges of electron density, temperature and emitter-perturber reduced mass. An equation is derived for n_e based on the full-width at half-maximum (FWHM) of H_β Stark broadening profile [32].

$$w_s = 4.8 \text{ nm} \left(\frac{n_e}{10^{17} cm^{-3}} \right)^{0.68116} \tag{5}$$

The Stark broadening of H_β line facilitates the n_e determination in atmospheric-pressure plasmas. High-spectrum resolution (e.g., 10 pm) is recommended for capturing a clear shape of the H_β line profile since other broadenings including Doppler, van der Waals, and instrumental broadenings contribute also to the detected line profile. The effects of these broadenings need to be separated to obtain the Stark part and accurate deconvolution procedures normally are required for this purpose [33]. Other atomic lines are also possible for n_e measurement based on their Stark broadening if hydrogen gas is absent, for example, He (447.1 nm) or Ar (415.9 nm) lines [34, 35].

Microwave interferometry and CO_2-laser heterodyne interferometry have been applied as well to n_e measurement in plasmas based on the principle of change in

refractive index of electromagnetic radiation passing through the discharge region [36, 37]. The main advantage of this technique is that it is able to measure electron densities at order of 10^{13} cm^{-3} lower than that by the Hβ Stark line broadening. However, since it is a line-integrated method and thermal effect may contribute also to the detected phase shift of probed electromagnetic radiation. This issue can be solved by using two laser sources with different wavelength [36]. Abel inversion is necessary to obtain spatially resolved electron density.

Compared to above two line-integrated techniques, Thomson scattering is a more advanced optical approach allows one probe directly information of both n_e and T_e [13]. This technique is based on the elastic scattering of light on free electrons, and its signal is Doppler broadened due to the velocity of electrons if the electron energy distribution function (EEDF) is a Maxwell-Boltzmann distribution. Therefore, n_e is able to be determined from the measured scattered power per unit of wavelength S_λ [38]:

$$\mathrm{S}_\lambda = \mathrm{C}n_e \frac{\mathrm{d}\sigma}{\mathrm{d}\Omega} \mathrm{G}_\lambda(\lambda) \tag{6}$$

where $C = flI_l\Delta\Omega$ is a constant factor depending on the optics efficiency f, length of detection volume l, laser power I_l, and detection solid angle $\Delta\Omega$. Absolute calibration needs to be done to determine the C value normally by means of Raman scattering on ambient air at atmospheric-pressure and room temperature [13]. $\mathrm{d}\sigma/\mathrm{d}\Omega$ is the differential cross section and $\mathrm{G}_\lambda(\lambda)$ is the function of spectral distribution and normalized normally that $\int \mathrm{G}_\lambda(\lambda)\mathrm{d}\lambda = 1$. T_e can be obtained by the measured Gaussian profile of Thomson scattering signal according to [13, 39]:

$$\mathrm{T}_e = \frac{m_e c^2}{4k_B} \left(\frac{\Delta\lambda}{\lambda_l}\right)^2 \tag{7}$$

$\Delta\lambda$ is the $1/e$ width of the Gaussian profile. Although these advantages of this advanced diagnostic technique, its implementation is not straightforward in general due to the weak scattered signal typically orders of magnitude lower than that of Rayleigh scattering in addition to stray light. A notch filter or a triple grating spectrometer, or an atomic absorption cell, are necessary to capture the weak scattered light [40–42]. And, laser-induced optical effects such as photo-detachment, photon-ionization, or electron heating may occur if high laser power is used in measurements, and need to be checked by measuring the signal as a function of laser power. More details about the Thomson scattering approach can be found in [13, 39, 41, 43–48].

3. Diagnostics of plasma chemistry (reactive species)

Plasma chemistry covers broad ranges of chemical properties of discharge plasmas, and rapidly grows to an important research area of scientific endeavor holding great promise for many novel plasma applications. Reactive species, including neutrals, metastable or excited species, ions consist the dominant active agents of discharges and play critical roles in plasma treatments, e.g., in fields of medicine, material, energy, etc. Various diagnostic techniques have been developed and applied for probing different reactive species quantitatively. And in this chapter three important techniques based on principles of laser-induced fluorescence (LIF) and absorption spectroscopy, are included.

3.1 Laser-induced fluorescence spectroscopy

Laser-induced fluorescence (LIF) is an *in situ* sensitive technique monitoring transient species with high temporal and spatial resolution [49]. This approach is based on a two-step process, where atoms or molecules in the initial electronic state i are firstly pumped to an upper electronic state j by absorbing laser photons with energy $\Delta E = h\upsilon_{ij}$ same to the transition gap between states i and j. Secondly, the excited state j undergoes spontaneous transition to a lower state k and emits photons with energy $h\upsilon_{jk}$ called the fluorescence signal. As an example, a conceptual LIF scheme of OH radicals, one typical reactive molecular species studied frequently by this technique, is depicted in **Figure 3**. For molecules fast vibrational energy transfer (VET) and rotational energy transfer (RET) processes are occurring after laser excitation, as well as the pre-dissociation process.

For atomic species these ro-vibrational processes are not existent. Although LIF is a direct technique allows us detect the spatial distributions of interested species, absolute calibration and analysis model are required for quantitative measurements [50–54]. For the case of single-photon excitation the fluorescence calibration is relative simple with the aid of Rayleigh scattering. It is based on a comparison under identical conditions of laser irradiation in Rayleigh scattering and fluorescence detection in LIF. A reference gas with known density is usually used for Rayleigh calibration, for instance air gas under room temperature. Typical laser excitations and fluorescence transitions of various species are listed in **Table 2** together with suggested calibration.

Analysis of fluorescence signal for absolutely determining probed species density can be very complicated under high gas pressure due to the fast collisional processes [67]. In this case the excited state after laser pumping may redistribute because of fast collisions at same timescale or even faster and these processes have to be considered in the analysis model. This could be more complicated for molecular species, for instance OH, NO, etc. in addition to the fast processes of VET and

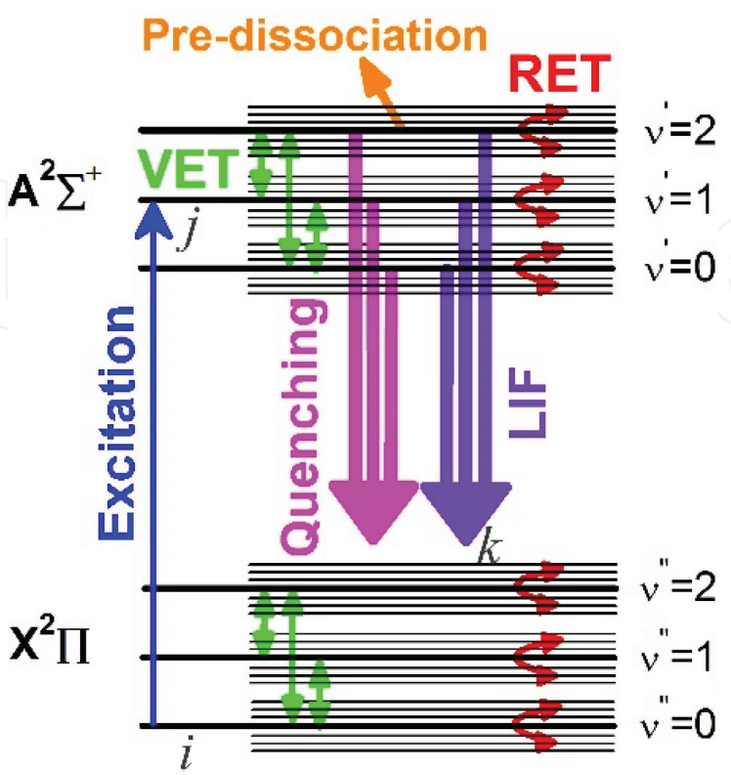

Figure 3.
LIF scheme of OH radicals.

Species	Excitation transition	Fluorescence transition	Calibration	Ref.
OH	$X^2\Pi$, v = 0 → $A^2\Sigma^+$, v = 1 283 nm	$A^2\Sigma^+$, v = 0 → $X^2\Pi$, v = 0 308 nm	Rayleigh of air	[50–54]
NO	$X^2\Pi$, v = 0 → $A^2\Sigma^+$, v = 0 226 nm	$A^2\Sigma^+$, v = 2 → $X^2\Pi$, v = 0 247 nm	NO gas	[55–59]
$N_2(A^3\Sigma_u^+)$	$A^3\Sigma_u^+$, v = 0 → $B^3\Pi_g$, v = 4 618 nm	$B^3\Pi_g$, v = 4 → $A^3\Sigma_u^+$, v = 1 678 nm	Rayleigh	[60–62]
NH	$X^3\Sigma^-$, v = 0 → $A^3\Pi_i$, v = 0 334 nm	$A^3\Pi_i$, v = 0 → $X^3\Sigma^-$, v = 0 336 nm	Rayleigh	[63, 64]
CH	$X^2\Pi$, v = 0 → $A^2\Delta$, v = 1 364 nm	$A^2\Delta$, v = 0 → $X^2\Pi$, v = 0 405 nm	Rayleigh	[65, 66]

Table 2.
The plasma species have been measured by single-photon LIF.

Species	Excitation wavelength (nm)	Fluorescence wavelength (nm)	Calibration	Ref.
O	225	845	Xe gas	[49, 73]
H	205	656	Kr gas	[74]
N	206	742–747	Kr gas	[75]
F	170	420	Ar gas	[49]
C	246	477	Rayleigh	[49]

Table 3.
Excitation schemes of various atomic species by TA-LIF technique.

RET [49]. Assumptions are often made for simplifying the LIF model, e.g., RET is fast enough to redistribute the rotational manifold of excited vibrational state and in this case the lifetime of the vibrational band can be considered only depending on quenching and emission coefficients. Effective lifetime of excited vibrational band instead of single rotational level, is used in the LIF model. And this is normally correct if RET process is fast, but still need to check if concentrations of quenching species such as H_2O to OH is very high [54, 68–70]. Furthermore, the laser power needs to be kept low and linear LIF is achieved to avoid stimulated emission and large depletion of initial pumped state density.

In many cases the excitation radiations locate range of deep UV (e.g., <100 nm) and are strongly absorbed by ambient gaseous medium (e.g., air or water molecules), then two-photon excitation in the UV spectral range (>200 nm) can be applied for the same diagnostic purpose, namely the so-called two-photon absorption LIF (TA-LIF) [49]. Compared to single-photon LIF, TA-LIF is considerably less efficient and the excitation rate scales with the square of laser power. Normally higher laser power is required to produce detectable fluorescence intensity, but laser stimulated effects including photon-ionization, induced breakdown, stimulated emission, etc. needs to be avoided [71, 72]. **Table 3** lists excitation schemes of TA-LIF for various active atomic species in plasmas. An example of two-dimensional distribution of atomic oxygen in an atmospheric-pressure plasma jet-source by TA-LIF is presented in **Figure 4**.

3.2 Absorption spectroscopy

Another important diagnostic technique for atmospheric-pressure plasmas is absorption spectroscopy (AS) [77]. Compared to LIF or OES approaches, AS is an *in*

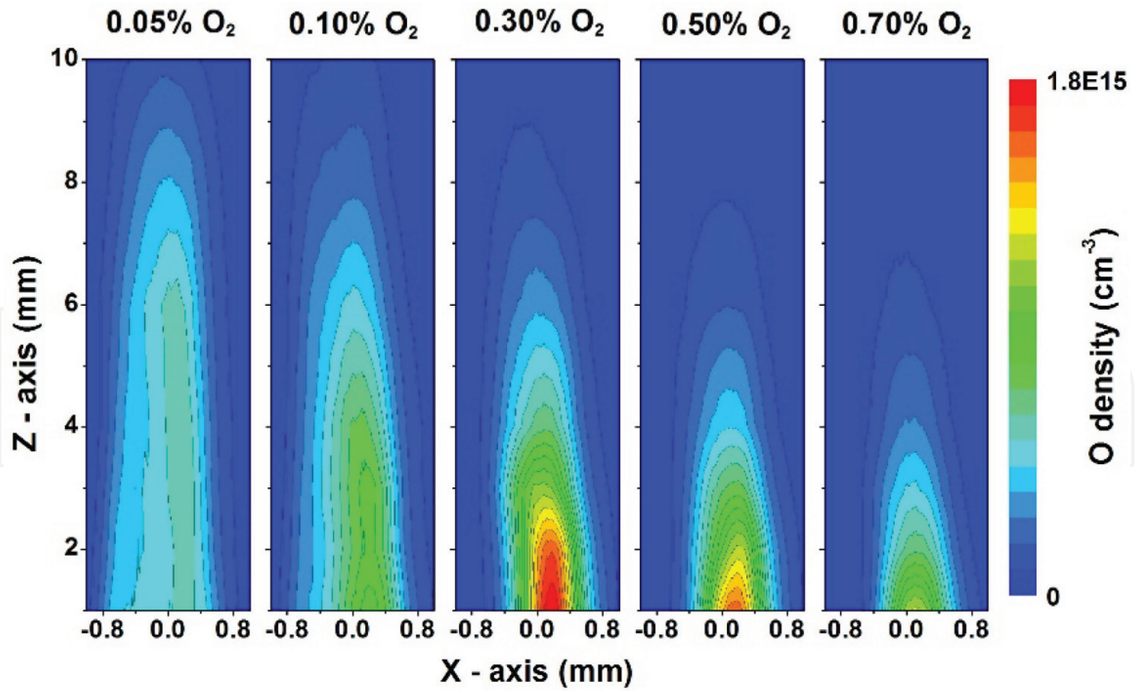

Figure 4.
Two-dimensional spatial distributions of ground-state O density in the x-z plane of the RF argon plasma jet under different O_2 admixtures [76].

situ and non-invasive technique probing absolute densities of interested species without need of extra calibration and independent on collisional quenching process. It relies on the *Beer-Lambert* law:

$$\mathrm{A}(\lambda) = -\ln\left(\frac{I_s}{I_0}\right) = \mathrm{N}\sigma(\lambda)\mathrm{L} \tag{8}$$

where I_s is the light intensity passing through sample, I_0 is the incident radiation, N is species density, $\sigma(\lambda)$ is the wavelength dependent absorption cross-section, and L is the absorption path-length. If probed species density is low, the absorption length is normally increased by using a multi-pass spectroscopic absorption cell where light reflects between two mirrors, e.g., the *Herriott* cell [78]. However, if for micro-plasmas this technique maybe not sensitive enough if species density is not high to obtain a distinct absorbance signal.

The sensitivity of absorption measurements is strongly dependent on the stability of used light source. Various types of light sources, narrow-band or broadband with wavelength range from VUV to mid-infrared, are applied together with high spectral resolution detection system such as spectrometer or FTIR. AS by laser light sources, particularly tunable diode-lasers or quantum cascade lasers are attractive light sources have been applied to measure species densities in micro-plasmas [8, 79, 80]. These laser sources output specific wavelengths of large absorption cross-sections and enable fine scan of wavelength to obtain a clear absorption line profile, and from which species density and even gas temperature are able to be derived.

Wavelength selectivity is important in the implementation of AS technique as absorption may overlap by multi-species. And, it should be mentioned that absorption measurements yield line-integrated densities and spatial distribution is achievable by Abel inversion. Special efforts are required for non-uniform micro-plasmas by AS approach, since gas temperature and species density are spatially dependent. In this case broadband absorption can provide more details for deriving both the gas

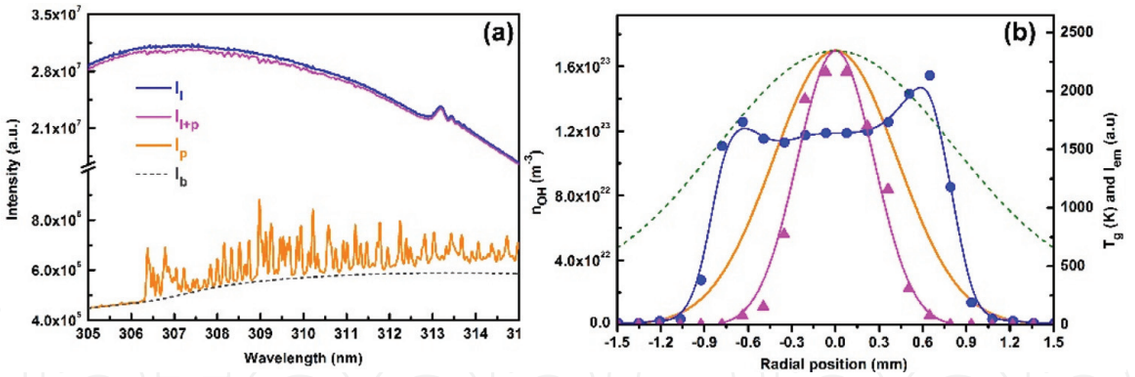

Figure 5.
(a) Measured spectra in the range 305–315 nm from the lamp source I_l, lamp and plasma on I_{l+p}, plasma on I_p, and the background I_b. (b) Radial profiles of OH density and gas temperature, and n(A-X) emission with or without filter from the cathode region of water-cathode discharge [83].

temperature and species density [81, 82]. An example of OH density determination by broadband UV absorption in an atmospheric-pressure pin-to-water discharge is depicted in **Figure 5** [83].

Another quite sensitive approach by using a cavity of two highly reflective mirrors is the cavity ring-down spectroscopy (CRDS) [84]. The laser pulse goes-and-back in the cavity and that effectively enhances the absorption path length in the probed gas sample by several orders of magnitude. The time-decay of light intensity leaking from the cavity depends on the reflectivity of mirrors and species density in the cavity. Based on that the species density is able to be obtained with the known mirror reflectivity. In addition to the high sensitivity, compared to absorption spectroscopy, CRDS is independent on fluctuations of light intensity since a time constant rather than an absolute absorbance is measured. More details of CRDS technique are included in Refs. [84-90].

4. Summary

High-end diagnostic techniques have been applied to atmospheric-pressure plasmas. Even for highly transient non-uniform micro-plasmas, reliable insights of discharge properties are able to be achieved. This chapter includes several important advanced diagnostic approaches specifically for plasma parameters and reactive plasma species. Two approaches are suggested for a same diagnostic purpose, for example, the determination of gas temperature or electron density, and compared to ensure and increase the measurement accuracy, particularly for atmospheric-pressure plasmas. Other important plasma properties, such as densities of ion species and ion flux, surface charges, have been investigated as well and related diagnostic techniques can be found in above (review) references.

Author details

Qing Xiong
State Key Laboratory of Power Transmission Equipment and System Security and New Technology, Chongqing University, Chongqing, China

*Address all correspondence to: qingugent@gmail.com

IntechOpen

References

[1] Wertheimer MR, Ahlawat M, Saoudi B, Kashyap R. Accurate in-situ gas temperature measurements in dielectric barrier discharges at atmospheric pressure. Applied Physics Letters. 2012; **100**(20):201112

[2] Bruggeman P, Sadeghi N, Schram D, Linss V. Gas temperature determination from rotational lines in non-equilibrium plasmas: A review. Plasma Sources Science and Technology. 2014;**23**(2): 023001

[3] Bruggeman P, Verreycken T, Gonzalez MA, Walsh JL, Kong MG, Leys C, et al. Optical emission spectroscopy as a diagnostic for plasmas in liquids: Opportunities and pitfalls. Journal of Physics D: Applied Physics. 2010; **43**(12):124005

[4] Luque J, Crosley D. LIFBASE: Database and spectral simulation (version 1.9). SRI International Report MP. 1999. 99-009

[5] http://www.specair-radiation.net [database on the Internet]

[6] Bruggeman PJ, Kushner MJ, Locke BR, Gardeniers JGE, Graham WG, Graves DB, et al. Plasma–liquid interactions: A review and roadmap. Plasma Sources Science and Technology. 2016;**25**(5):053002

[7] Xiong Q, Nikiforov AY, Lu XP, Leys C. High-speed dispersed photographing of an open-air argon plasma plume by a grating–ICCD camera system. Journal of Physics D: Applied Physics. 2010; **43**(41):415201

[8] Bol'shakov AA, Cruden BA, Sharma SP. Determination of gas temperature and thermometric species in inductively coupled plasmas by emission and diode laser absorption. Plasma Sources Science and Technology. 2004;**13**(4): 691-700

[9] Jackson GP, King FL. Probing excitation/ionization processes in millisecond-pulsed glow discharges in argon through the addition of nitrogen. Spectrochimica Acta B. 2003;**58**(2): 185-209

[10] Xiong Q, Xu L, Wang X, Xiong L, Huang Q, Chen Q, et al. Full spatial-field visualization of gas temperature in an air micro-glow discharge by calibrated Schlieren photography. Journal of Physics D: Applied Physics. 2018;**51**(9):095207

[11] Miles RB, Lempert WR, Forkey JN. Laser Rayleigh scattering. Measurement Science and Technology. 2001;**12**(5): R33-R51

[12] Adams SF, Caplinger JE, Sommers BS. Spatial temperature mapping of an atmospheric microdischarge using ultraviolet Rayleigh scatter imaging. Plasma Sources Science and Technology. 2015;**24**(2):025031

[13] van Gessel AH, Carbone ED, Bruggeman P, van der Mullen JM. Laser scattering on an atmospheric pressure plasma jet: Disentangling Rayleigh. Raman and Thomson scattering. Plasma Sources Science and Technology. 2012; **21**(1):015003

[14] Verreycken T, van Gessel A, Pageau A, Bruggeman P. Validation of gas temperature measurements by OES in an atmospheric air glow discharge with water electrode using Rayleigh scattering. Plasma Sources Science and Technology. 2011;**20**(2):024002

[15] Hargather MJ, Settles GS. A comparison of three quantitative Schlieren techniques. Optics and Lasers in Engineering. 2012;**50**(1):8-17

[16] Settles GS, Hargather MJ. A review of recent developments in Schlieren and

shadowgraph techniques. Measurement Science and Technology. 2017;**28**(4): 042001

[17] Ishino Y, Hayashi N, Bt Abd Razak IF, Kato T, Kurimoto Y, Saiki Y. 3D-CT (computer tomography) measurement of an instantaneous density distribution of turbulent flames with a multi-directional quantitative Schlieren camera (reconstructions of high-speed premixed burner flames with different flow velocities). Flow, Turbulence and Combustion. 2016;**96**(3):819-835

[18] Ionascut-Nedelcescu A, Carlone C, Kogelschatz U, Gravelle DV, Boulos MI. Calculation of the gas temperature in a throughflow atmospheric pressure dielectric barrier discharge torch by spectral line shape analysis. Journal of Applied Physics. 2008;**103**(6):063305

[19] Yubero C, Dimitrijević MS, García MC, Calzada MD. Using the van der Waals broadening of the spectral atomic lines to measure the gas temperature of an argon microwave plasma at atmospheric pressure. Spectrochimica Acta B. 2007;**62**(2):169-176

[20] Qing X, Le X, Lin X, Qinghua H, Qiang C, Yi C, et al. Heat deposition in the thermal field of a micro-glow discharge: Effect of humidity. Plasma Sources Science and Technology. 2018; **27**(9):095010

[21] Tobin JD, Hargather MJ. Quantitative Schlieren measurement of explosively-driven shock wave density, temperature, and pressure profiles. Propellants, Explosives, Pyrotechnics. 2016;**41**(6):1050-1059

[22] Ito T, Kobayashi K, Mueller S, Luggenhölscher D, Czarnetzki U, Hamaguchi S. Electric field measurement in an atmospheric or higher pressure gas by coherent Raman scattering of nitrogen. Journal of Physics D: Applied Physics. 2009;**42**(9):092003

[23] Ochkin VN, Savinov SY, Tskhai SN, Czarnetzki U, Gathen VS, Dobele HF. Nonlinear optical techniques for plasma diagnostics. IEEE Transactions on Plasma Science. 1998;**26**(5):1502-1513

[24] Ito T, Kanazawa T, Hamaguchi S. Rapid breakdown mechanisms of open air nanosecond dielectric barrier discharges. Physical Review Letters. 2011;**107**(6):065002

[25] Ito T, Kobayashi K, Czarnetzki U, Hamaguchi S. Rapid formation of electric field profiles in repetitively pulsed high-voltage high-pressure nanosecond discharges. Journal of Physics D: Applied Physics. 2010;**43**(6): 062001

[26] Simeni MS, Baratte E, Zhang C, Frederickson K, Adamovich IV. Electric field measurements in nanosecond pulse discharges in air over liquid water surface. Plasma Sources Science and Technology. 2018;**27**(1):015011

[27] Simeni MS, Goldberg B, Gulko I, Frederickson K, Adamovich IV. Sub-nanosecond resolution electric field measurements during ns pulse breakdown in ambient air. Journal of Physics D: Applied Physics. 2017;**51**(1): 01LT01

[28] Simeni Simeni M, Goldberg BM, Zhang C, Frederickson K, Lempert WR, Adamovich IV. Electric field measurements in a nanosecond pulse discharge in atmospheric air. Journal of Physics D: Applied Physics. 2017;**50**(18): 184002

[29] Simeni Simeni M, Tang Y, Frederickson K, Adamovich IV. Electric field distribution in a surface plasma flow actuator powered by ns discharge pulse trains. Plasma Sources Science and Technology. 2018;**27**(10):104001

[30] Gigosos MA, Cardenoso V. Study of the effects of ion dynamics on Stark profiles of Balmer-α and -β lines using

simulation techniques. The Journal of Physics B: Atomic, Molecular and Optical Physics. 1987;**20**(22):6005-6019

[31] Ivković M, Jovićević S, Konjević N. Low electron density diagnostics: Development of optical emission spectroscopic techniques and some applications to microwave induced plasmas. Spectrochimica Acta B. 2004; **59**(5):591-605

[32] Gigosos MA, González MÁ, Cardeñoso V. Computer simulated Balmer-alpha, -beta and -gamma Stark line profiles for non-equilibrium plasmas diagnostics. Spectrochimica Acta B. 2003;**58**(8):1489-1504

[33] Bruggeman P, Schram D, González MÁ, Rego R, Kong MG, Leys C. Characterization of a direct dc-excited discharge in water by optical emission spectroscopy. Plasma Sources Science and Technology. 2009;**18**(2):025017

[34] Du B, Sadeghi N, Tsankov TV, Luggenhölscher D, Czarnetzki U. Temporally resolved optical emission spectroscopic investigations on a nanosecond self-pulsing micro-thin-cathode discharge. Plasma Sources Science and Technology. 2012;**21**(4): 045015

[35] Xiong Q, Nikiforov AY, González MÁ, Leys C, Lu XP. Characterization of an atmospheric helium plasma jet by relative and absolute optical emission spectroscopy. Plasma Sources Science and Technology. 2012;**22**(1):015011

[36] Choi J-Y, Takano N, Urabe K, Tachibana K. Measurement of electron density in atmospheric pressure small-scale plasmas using CO_2-laser heterodyne interferometry. Plasma Sources Science and Technology. 2009; **18**(3):035013

[37] Leipold F, Stark RH, El-Habachi A, Schoenbach KH. Electron density measurements in an atmospheric pressure air plasma by means of infrared heterodyne interferometry. Journal of Physics D: Applied Physics. 2000; **33**(18):2268-2273

[38] Kempkens H, Uhlenbusch J. Scattering diagnostics of low-temperature plasmas (Rayleigh scattering, Thomson scattering, CARS). Plasma Sources Science and Technology. 2000;**9**(4):492-506

[39] Muraoka K, Uchino K, Bowden MD. Diagnostics of low-density glow discharge plasmas using Thomson scattering. Plasma Physics and Controlled Fusion. 1998;**40**(7): 1221-1239

[40] Jia F, Sumi N, Ishikawa K, Kano H, Inui H, Kularatne J, et al. Laser scattering diagnosis of a 60-Hz non-equilibrium atmospheric pressure plasma jet. Applied Physics Express. 2011;**4**(2):026101

[41] Muraoka K, Kono A. Laser Thomson scattering for low-temperature plasmas. Journal of Physics D: Applied Physics. 2011;**44**(4):043001

[42] Sande MJ, Deckers RHM, Lepkojus F, Buscher W, Mullen JJAM. Time resolved electron density and temperature measurements on a capacitively coupled helium RF discharge. Plasma Sources Science and Technology. 2002;**11**(4):466-475

[43] Nedanovska E, Nersisyan G, Morgan TJ, Hüwel L, Lewis CLS, Riley D, et al. Comparison of the electron density measurements using Thomson scattering and emission spectroscopy for laser induced breakdown in one atmosphere of helium. Applied Physics Letters. 2011;**99**(26):261504

[44] Hassaballa S, Yakushiji M, Young-Kee K, Tomita K, Uchino K, Muraoka K. Two-dimensional structure of PDP micro-discharge plasmas obtained using laser Thomson scattering. IEEE

Transactions on Plasma Science. 2004; **32**(1):127-134

[45] Noguchi Y, Matsuoka A, Bowden MD, Uchino K, Muraoka K. Measurements of electron temperature and density of a micro-discharge plasma using laser Thomson scattering. Japanese Journal of Applied Physics. 2001;**40**(1(1)):326-329

[46] Kono A, Iwamoto K. High-spatial-resolution multichannel Thomson scattering measurements for atmospheric pressure microdischarge. Japanese Journal of Applied Physics. 2004;**43**(8A):L1010-L10L3

[47] Palomares JM, Iordanova E, Hübner S, Carbone EAD, JJAMvd M. Towards poly-diagnostics on cool atmospheric plasmas. Journal of Instrumentation. 2012;**7**(02):C02027-C

[48] Kempkens H, Uhlenbusch J. Scattering diagnostics of low-temperature plasmas (Rayleigh scattering, Thomson scattering, CARS). Plasma Sources Science and Technology. 2000;**9**:492

[49] Döbele H, Mosbach T, Niemi K, Gathen V. Laser-induced fluorescence measurements of absolute atomic densities: Concepts and limitations. Plasma Sources Science and Technology. 2005;**14**(2):S31-S41

[50] Dilecce G, Ambrico PF, Benedictis SD. An ambient air RF low-pressure pulsed discharge as an OH source for LIF calibration. Plasma Sources Science and Technology. 2004;**13**(2):237-244

[51] Dilecce G, Ambrico PF, Simek M, De Benedictis S. LIF diagnostics of hydroxyl radical in atmospheric pressure He-H_2O dielectric barrier discharges. Chemical Physics. 2012;**398**: 142-147

[52] Riès D, Dilecce G, Robert E, Ambrico P, Dozias S, Pouvesle J. LIF and fast imaging plasma jet characterization relevant for NTP biomedical applications. Journal of Physics D: Applied Physics. 2014;**47**(27):275401

[53] Verreycken T, van der Horst R, Baede A, Veldhuizen V, Bruggeman P. Time and spatially resolved LIF of OH in a plasma filament in atmospheric pressure He–H_2O. Journal of Physics D: Applied Physics. 2012;**45**(4):045205

[54] Yagi I, Ono R, Oda T, Takaki K. Two-dimensional LIF measurements of humidity and OH density resulting from evaporated water from a wet surface in plasma for medical use. Plasma Sources Science and Technology. 2015;**24**(1): 015002

[55] Iseni S, Zhang S, van Gessel AFH, Hofmann S, van Ham BTJ, Reuter S, et al. Nitric oxide density distributions in the effluent of an RF argon APPJ: Effect of gas flow rate and substrate. New Journal of Physics. 2014;**16**(12): 123011

[56] Burnette D, Shkurenkov I, Adamovich IV, Lempert WR. Kinetics of NO formation and decay in nanosecond pulse discharges in air, H_2-air, and C_2H_4-air mixtures. Plasma Sources Science and Technology. 2016; **25**(2):025012

[57] Dilecce G, Ambrico PF, Šimek M, De Benedictis S. New laser-induced fluorescence scheme for simultaneous OH and NO detection by a single laser set-up. Applied Physics B: Lasers and Optics. 2002;**75**(1):131-135

[58] van Gessel AFH, Hrycak B, Jasiński M, Mizeraczyk J, van der Mullen JJAM, Bruggeman PJ. Temperature and NO density measurements by LIF and OES on an atmospheric pressure plasma jet. Journal of Physics D: Applied Physics. 2013;**46**(9):095201

[59] van Gessel AFH, Bruggeman PJ. Thermalization of rotational states of

NO $A(2)\Sigma^+(v = 0)$ in an atmospheric pressure plasma. The Journal of Chemical Physics. 2013;**138**(20):204306

[60] Simek M, Ambrico P, Prukner V. LIF study of $N_2(A^3\Sigma_u^+, v = 0–10)$ vibrational kinetics under nitrogen streamer conditions. Journal of Physics D: Applied Physics. 2015;**48**(26):265202

[61] Simek M, Ambrico P, Prukner V. $N_2(A)$ vibrational kinetics in streamer discharges: Effect of oxygen on formation of low vibrational levels. APS Gaseous Electronics Conference 2016. Bochum 2016

[62] Ono R, Tobaru C, Teramoto Y, Oda T. Laser-induced fluorescence of $N_2(A^3\Sigma_u^+)$ metastable in N_2 pulsed positive corona discharge. Plasma Sources Science and Technology. 2009; **18**(2):025006

[63] Brackmann C, Zhou B, Li ZS, Aldén M. Strategies for quantitative planar laser-induced fluorescence of NH radicals in flames. Combustion Science and Technology. 2016;**188**(4–5):529-541

[64] Rensberger KJ, Dyer MJ, Wise ML, Copeland RA. Time-resolved laser-induced fluorescence in low-pressure flames. AIP Conference Proceedings. 1988;**172**(1):750-752

[65] Luque J, Klein-Douwel RJH, Jeffries JB, Smith GP, Crosley DR. Quantitative laser-induced fluorescence of CH in atmospheric pressure flames. Applied Physics B: Lasers and Optics. 2002; **75**(6):779-790

[66] Luque J, Crosley DR. Absolute CH concentrations in low-pressure flames measured with laser-induced fluorescence. Applied Physics B: Lasers and Optics. 1996;**63**(1):91-98

[67] Bruggeman P, Brandenburg R. Atmospheric pressure discharge filaments and microplasmas: Physics, chemistry and diagnostics. Journal of Physics D: Applied Physics. 2013; **46**(46):464001

[68] Yagi I, Shirakawa Y, Hirakata K, Akiyama T, Yonemori S, Mizuno K, et al. Measurement of OH, O, and NO densities and their correlations with mouse melanoma cell death rate treated by a nanosecond pulsed streamer discharge. Journal of Physics D: Applied Physics. 2015;**48**(42):424006

[69] Yonemori S, Nakagawa Y, Ono R, Oda T. Measurement of OH density and air–helium mixture ratio in an atmospheric-pressure helium plasma jet. Journal of Physics D: Applied Physics. 2012;**45**(22):225202

[70] Yonemori S, Ono R. Flux of OH and O radicals onto a surface by an atmospheric-pressure helium plasma jet measured by laser-induced fluorescence. Journal of Physics D: Applied Physics. 2014;**47**(12):125401

[71] Amorim J, Baravian G. The two-photon absorption laser induced stimulated emission as a hydrogen atoms diagnostic tool: Modelling and experiment. Optics Communications. 2001;**192**(3):277-286

[72] Amorim J, Baravian G, Touzeau M, Jolly J. Two-photon laser induced fluorescence and amplified spontaneous emission atom concentration measurements in O_2 and H_2 discharges. Journal of Applied Physics. 1994;**76**(3): 1487-1493

[73] Niemi K, Gathen VS-v, Döbele HF. Absolute atomic oxygen density measurements by two-photon absorption laser-induced fluorescence spectroscopy in an RF-excited atmospheric pressure plasma jet. Plasma Sources Science and Technology. 2005; **14**(2):375-386

[74] Yatom S, Luo Y, Xiong Q, Bruggeman PJ. Nanosecond pulsed humid Ar plasma jet in air: Shielding,

discharge characteristics and atomic hydrogen production. Journal of Physics D: Applied Physics. 2017;**50**(41):415204

[75] Wagenaars E, Gans T, O'Connell D, Niemi K. Two-photon absorption laser-induced fluorescence measurements of atomic nitrogen in a radio-frequency atmospheric-pressure plasma jet. Plasma Sources Science and Technology. 2012;**21**(4):042002

[76] Xiong Q, Liu H, Britun N, Nikiforov AY, Li L, Chen Q, et al. Time-selective TALIF spectroscopy of atomic oxygen applied to an atmospheric pressure argon plasma jet. IEEE Transactions on Plasma Science. 2016;**44**(11):2745-2753

[77] Reuter S, Sousa JS, Stancu GD, Hubertus van Helden JP. Review on VUV to MIR absorption spectroscopy of atmospheric pressure plasma jets. Plasma Sources Science and Technology. 2015;**24**(5):054001

[78] Reuter S, Winter J, Iseni S, Peters S, Schmidt-Bleker A, Dünnbier M, et al. Detection of ozone in a MHz argon plasma bullet jet. Plasma Sources Science and Technology. 2012;**21**(3): 034015

[79] Douat C, Hübner S, Engeln R, Benedikt J. Production of nitric/nitrous oxide by an atmospheric pressure plasma jet. Plasma Sources Science and Technology. 2016;**25**(2):025027

[80] Simeni Simeni M, Laux CO, Stancu GD. High-spatial resolution measurements of NO density and temperature by mid-IR QCLAS in open-air confined plasmas. Journal of Physics D: Applied Physics. 2017;**50**(27):274004

[81] Bruggeman P, Cunge G, Sadeghi N. Absolute OH density measurements by broadband UV absorption in diffuse atmospheric-pressure He–H_2O RF glow discharges. Plasma Sources Science and Technology. 2012;**21**(3):035019

[82] Dilecce G, Ambrico PF, Simek M, Benedictis SD. OH density measurement by time-resolved broad band absorption spectroscopy in an Ar–H_2O dielectric barrier discharge. Journal of Physics D: Applied Physics. 2012; **45**(12):125203

[83] Xiong Q, Yang Z, Bruggeman P. Absolute OH density measurements in an atmospheric pressure dc glow discharge in air with water electrode by broadband UV absorption spectroscopy. Journal of Physics D: Applied Physics. 2015;**48**(42):424008

[84] Berden G, Engeln R. Cavity Ring-Down Spectroscopy: Techniques and Applications. New York: Wiley; 2009

[85] Zalicki P, Zare RN. Cavity ring-down spectroscopy for quantitative absorption measurements. The Journal of Chemical Physics. 1995;**102**(7): 2708-2717

[86] Stancu GD, Janda M, Kaddouri F, Lacoste DA, Laux CO. Time-resolved CRDS measurements of the $N_2(A^3\Sigma_u^+)$ density produced by nanosecond discharges in atmospheric pressure nitrogen and air. Journal of Physical Chemistry C. 2010;**114**(1):201-208

[87] Stancu GD, Kaddouri F, Lacoste DA, Laux CO. Atmospheric pressure plasma diagnostics by OES, CRDS and TALIF. Journal of Physics D: Applied Physics. 2010;**43**(12):124002

[88] Liu Z-W, Xu Y, Yang X-F, Zhu A-M, Zhao G-L, Wang W-G. Determination of the HO_2 radical in dielectric barrier discharge plasmas using near-infrared cavity ring-down spectroscopy. Journal of Physics D: Applied Physics. 2008;**41**(4):045203

[89] Gianella M, Reuter S, Press SA, Schmidt-Bleker A, Helden JH, Ritchie GAD. HO_2 reaction kinetics in an atmospheric pressure plasma jet determined by cavity ring-down

spectroscopy. Plasma Sources Science and Technology. 2018;**27**(9):095013

[90] Wang C, Wu W. Simultaneous measurements of OH(A) and OH(X) radicals in microwave plasma jet-assisted combustion of methane/air mixtures around the lean-burn limit using optical emission spectroscopy and cavity ringdown spectroscopy. Journal of Physics D: Applied Physics. 2013; **46**(46):464008